Mapping of the Bak, Tang, and Wiesenfeld sandpile model on a two-dimensional Ising-correlated percolation lattice to the two-dimensional self-avoiding random walk

J. Cheraghalizadeh,[1,*] M. N. Najafi,[1,†] H. Dashti-Naserabadi,[2,‡] and H. Mohammadzadeh[1,§]
[1]*Department of Physics, University of Mohaghegh Ardabili, P.O. Box 179, Ardabil, Iran*
[2]*Physics and Accelerators Research School, NSTRI, AEOI 11365-3486, Tehran, Iran*
(Received 20 August 2017; revised manuscript received 14 October 2017; published 17 November 2017)

The self-organized criticality on the random fractal networks has many motivations, like the movement pattern of fluid in the porous media. In addition to the randomness, introducing correlation between the neighboring portions of the porous media has some nontrivial effects. In this paper, we consider the Ising-like interactions between the active sites as the simplest method to bring correlations in the porous media, and we investigate the statistics of the BTW model in it. These correlations are controlled by the artificial "temperature" T and the sign of the Ising coupling. Based on our numerical results, we propose that at the Ising critical temperature T_c the model is compatible with the universality class of two-dimensional (2D) self-avoiding walk (SAW). Especially the fractal dimension of the loops, which are defined as the external frontier of the avalanches, is very close to $D_f^{\mathrm{SAW}} = \frac{4}{3}$. Also, the corresponding open curves has conformal invariance with the root-mean-square distance $R_{\mathrm{rms}} \sim t^{3/4}$ (t being the parametrization of the curve) in accordance with the 2D SAW. In the finite-size study, we observe that at $T = T_c$ the model has some aspects compatible with the 2D BTW model (e.g., the $1/\log(L)$-dependence of the exponents of the distribution functions) and some in accordance with the Ising model (e.g., the $1/L$-dependence of the fractal dimensions). The finite-size scaling theory is tested and shown to be fulfilled for all statistical observables in $T = T_c$. In the off-critical temperatures in the close vicinity of T_c the exponents show some additional power-law behaviors in terms of $T - T_c$ with some exponents that are reported in the text. The spanning cluster probability at the critical temperature also scales with $L^{\frac{1}{2}}$, which is different from the regular 2D BTW model.

DOI: 10.1103/PhysRevE.96.052127

I. INTRODUCTION

The notion of critical phenomena on the fractal lattices is a long-standing problem in the literature. Gefen *et. al.* were the first who systematically studied the problem [1]. Experimental motivations for such a study can be found in some works like Refs. [2–8], in which the voids of percolating clusters were filled by (commonly magnetite) nanoparticles of a ferromagnetic fluid. For such problems the Ising model in the percolation clusters is the best and simplest realization [9] (should not be confused with the Ising model as the metric space in the current paper). There are also some other dynamical processes in the fractal systems, such as the propagation of fluids in the reservoirs in the displacement method of the oil recovery. In this approach, the water or the gas is injected into a well so that the percolation theory (as the host space) can be employed to find the percentage of the injected fluid which is percolated to the production well [10]. This movement shows degrees of (self-organized) criticality [11,12], which can be shown by employing the Darcy model [13] as a powerful tool that has the potential to bring most parameters of the reservoirs in the calculations [14]. Such natural processes have the chance to be described in terms of self-organized criticality (SOC), which is a large class of critical phenomena containing the systems that organize themselves in a critical state. The concept was invented by Bak, Tang, and Wiesenfeld [18,19] (known as the BTW model) who mentioned that this self-organization needs some energy input and output to be balanced and explained the well-known $1/f$ noise in the natural processes. The connection of the reservoirs with the SOC was made by connecting the water saturation threshold in the Darcy model, and the critical height in the sandpile model. The other important example of the SOC on the random systems is the experiment by Beggs *et al.* [15], in which it was shown that the propagation of spontaneous activity in cortical networks is self-organized critical phenomena described by neuronal avalanches just like the sandpile models. This motivates one to theoretically investigate the sandpile models in the random networks [16] and in the two- and three-dimensional small-world networks [17] as the models for the neuronal activity. Many analytical and theoretical aspects of the BTW model are known [20–24], containing different height and cluster probabilities [25], avalanche distribution [26–28], the connection of the model to spanning trees [29], ghost models [30], and q-state Potts model [31,32]. For a good review see Ref. [33]. One of the first examples of the SOC phenomena on the fractal lattices was mentioned by Najafi *et al.*, who realized the movement pattern of fluid in the two-dimensional (2D) porous media by implementing the BTW model on the 2D uncorrelated percolation lattice [34,35]. The most important reason for this connection was claimed to be the existence of the *saturation threshold* phenomenon in the real porous media, which was realized by the toppling threshold in the BTW model on the percolation lattice [34]. It was also claimed that this model right at the percolation threshold corresponds to the

*jafarcheraghalizadeh@gmail.com
†morteza.nattagh@gmail.com
‡h.dashti82@gmail.com
§h.mohammadzadeh@gmail.com

Ising universality class [34,35], which is consistent with the results of the geometrical properties of the Darcy's reservoir model [13]. Especially the fractal dimension of the frontier of the avalanches was shown to be compatible with the fractal dimension of the geometrical spin clusters of the critical Ising model $D_F = \frac{11}{8}$. By using the Schramm-Loewner evolution technique, it has also been shown that this model is consistent with the Ising model with the diffusivity parameter $\kappa = 3$. All of these results show that the BTW model is a good candidate for simulating the movement pattern of the fluid in the porous media. This becomes more worthy when one considers the fact that the other common statistical models, such as invasion percolation [36], do not include the saturation threshold for overflowing of the fluid to the neighboring regions. The BTW on the three-dimensional uncorrelated percolation lattice is the more realistic problem, which is done in Ref. [17], in which it is shown that the exponents out of the percolation threshold $p > p_c$ is logarithmically corrected in terms of $p - p_c$.

The realization of the porous media with the uncorrelated percolation lattice seems to be *ad hoc*, since the permeable pores of the porous media are not completely independent in the natural systems. As an example, consider the sedimentation process of the reservoir rock in which some parts of the reservoir rock become impermeable to flow [14]. This usually happens because of some impermeable objects, such as shale bodies, resulting to the formation of *unoccupied* or *inactive* sites in the porous media. Therefore, the correlation of the unoccupied sites depends on the dynamics of the sedimentation process. Many models to bring the spatial correlations in the simulations have been proposed. For example, a long-range correlation was considered in Ref. [37] that comes from fracture surfaces. Also, in Ref. [38], correlations are considered by fractional Brownian motion. More recently, a finite-range correlation was also studied and the effect on the drying process of the correlation length was investigated [39]. The aim of the present paper is to realize the dynamics of the fluid by means of the BTW model and take the spatial correlations [of occupied (or unoccupied) sites] into account by minimally manipulating the percolation theory. One (and presumably easiest) way to model the correlations in the (porous) host media is to use the Ising interactions. If we choose ferromagnetic interactions, then in the original model the occupied sites have constructive correlations, meaning that two disjoint impermeable regions favor to get closer to each other, or equivalently impermeable rocks absorb each other in the sedimentation processes. In the antiferromagnetic case, however, the interactions are repulsive. We model the correlation of the occupied sites by the ferromagnetic Ising model. In this approach, a site can have two states: occupied and unoccupied corresponding to spin up and spin down states in the dual Ising model respectively. The strength of the correlations is controlled by the Ising coupling constant and the artificial *temperature* T. Therefore by varying the artificial temperature, we actually control the correlations and the ordinary uncorrelated percolation system is expected to be reached as the temperature goes to infinity. Our results show that at $T = T_c$ the self-avoiding universality class is obtained. Also the exponents near the critical temperature show additional power-law behaviors in terms of $T - T_c$.

Mixing of two conformal symmetric models is also of interest in the theoretical side. Mathematically this problem can be tracked in terms of the Zamolodchkiv's c-theorem, in which knowing the scaling perturbing filed, one can obtain the change of central charge of the conformal field theory $\delta c = c_{\rm IR} - c_{\rm UV}$ [40]. In this language the effect of the second CFT model can presumably codded in a scaling field from the operator content of the original (first) CFT model, which we name the perturbing field. However, this approach is not practical for the less-known models since determining the structure of the renormalization group flows minimally needs the knowledge of the perturbing field, which is generally not known. In these situations the statistical methods can be useful by which the critical model can be characterized and the corresponding universality class can be obtained.

The paper has been organized as follows: In Sec. II, we motivate this study and introduce and describe the model. The results are presented in Sec. III, which contains two subsections: Sec. III A, in which the critical results are presented, and Sec. III B, in which the power-law behaviors in the off-critical temperatures are presented. We end the paper with a conclusion in Sec. IV.

II. THE CONSTRUCTION OF THE PROBLEM

The dynamics of particles or spins in the porous media is the main motivation for the statistical models in the fractal lattices as the host. These host systems should involve some stochasticity to be a true realization of the real systems. Examples of the spin dynamics in the porous media can be found in Refs. [2–8], which are theoretically considered in Ref. [9], in which the porous media has been simulated as the uncorrelated percolation lattice. The dynamics of particles (and fluids in the continuum limit) in the porous media is more important in the petroleum engineering since the knowledge of the propagation pattern of the fluid in these systems is vital in extracting oil [34]. The similarity of some aspects of the local rules of the fluid propagation in real systems and the toppling rules in the sandpile models encourages one to apply the sandpile models in the percolation lattice as the realization of the porous media. It has been shown that some geometrical properties of the latter is similar to the ones for the real systems which is modeled by the Darcy's reservoir model, e.g., the fractal dimension of the frontiers of the avalanches in both cases is the same in $p = p_c$ and is equal to the loops of the spin clusters of the critical Ising model; i.e., $D_f^{\rm Ising} = \frac{11}{8}$ [13,34].

Considering the uncorrelated percolation lattice as the realization of the porous media is a crude assumption and may not be justified for all systems, since in the sedimentation process of the reservoir rocks, the impermeable objects can affect each other. To realize the interactions in the sedimentation process, one should use a two-state model with short range interactions, since the sedimentation (and generally the presence) of a rock can only affect its neighborhood sites in the close vicinity of that region. In the present paper we model the impermeability-permeability configuration of the rocks by the Ising model to realize the interactions and correlations in the sedimentation process. This assumption is not phenomenological and is a physical assumption regarding the interactions in sedimentation. It has three benefits: firstly it is a two-state

model, secondly it contains short-range interactions and thirdly it is simple for simulation. The spins of the employed Ising model play the role of the field of presence or absence of the permeable rocks. More precisely, if we show the spins by σ, then $\sigma = +1$ ($\sigma = -1$) are attributed to the permeable (impermeable) sites. The positive-correlated case is realized by the ferromagnetic Ising model (positive coupling constant), whereas the negative-correlated case is realized by the antiferromagnetic one (negative coupling constant). The correlations of our zero-magnetic field Ising system is controlled by the temperature T which has nothing to do with the real temperature. Therefore, we should mention that T is an artificial temperature. We use this word without "artificial" throughout this paper, having in mind that we mean the control parameter, which tunes the correlations of the host system. To this end, we use the Ising Hamiltonian (H) in the zero magnetic field:

$$H = -J \sum_{\langle i,j \rangle} \sigma_i \sigma_j - h \sum_i \sigma_i, \quad \sigma_i = \pm 1, \tag{1}$$

in which J is the coupling constant, h is the magnetic field, and σ_i and σ_j are the spins at the sites i and j, respectively, having the values ∓ 1 (as introduced above). $\langle i,j \rangle$ shows that the sites i and j are neighbors. $J > 0$ corresponds to ferromagnetic system (positively correlated host lattice), whereas $J < 0$ is for antiferromagnetic ones (negatively correlated host lattice). We emphasize that in this paper we use the Ising model as the metric space and our model is not a magnetic one; instead, the spins show the state of the pores the porous media. The artificial temperature T controls the population of the permeable rocks relative to the total number of rocks and also controls the heterogeneity and correlations of the host system. On the other hand, h, which controls the preferred direction for the spins in the Ising model, shows the tendency of the porous media for having permeable ($h > 0$) or impermeable ($h < 0$) sites. For $h = 0$ the model is well-known to exhibit a nonzero magnetization per site $M = \langle \sigma_i \rangle$ at temperatures bellow the critical temperature T_c. Although we set $h = 0$ throughout this paper, we prefer to mention some points concerning this parameter here. In the Ising model the magnetization has a discontinuity at $h = 0$ along the $T < T_c$ line, i.e., for $h = 0^+$ and $T < T_c$ we have $M > 0$, whereas for the case $h = 0^-$ and $T < T_c$ we have $M < 0$. We can have a percolation description of the Ising model which is controlled by T and h as follows: In each T and h the system is composed of some spin clusters. Let us consider only up-spin clusters, having in mind that the system has the symmetry $h \to -h$ and $\sigma_i \to -\sigma_i$. We define $h_{th}(T)$ as the magnetic field threshold below which there is no spanning cluster of the parallel spins and above which some spanning clusters appear. Apparently, for $T = 0$ all spins align in the same direction and $H_{\rm th}(T = 0) = 0^+$. Also, for $T = \infty$ the spins are uncorrelated and take the up direction with the probability $\frac{1}{2}e^h / \cosh h$. Therefore, the percolation threshold $p_c^{\rm Ising}$ in the case $T \to \infty$ is

$$p_c^{\rm Ising} = \frac{e^{h_{\rm th}(\infty)}}{2\cosh\left[h_{\rm th}(\infty)\right]}. \tag{2}$$

Although this picture helps to understand the percolation aspects of the Ising model, it has nothing to do with the case $h = 0$. There are two transitions in the Ising model: the magnetic (paramagnetic to ferromagnetic) transition and the percolation transition (in which the connected geometrical spin clusters percolate). For the 2D regular Ising model at $h = 0$, these two transitions occur simultaneously [41], although it is not the case for all versions of the Ising model, e.g., for the site-diluted Ising model [9]. For the details of the percolation transition associated with the critical point of the 2D Ising model see Refs. [42] and [43].

Before describing the dynamics in this type of porous media, let us first briefly introduce the standard BTW model on a regular d-dimensional hypercubic lattice [18]; each site i has an integer height (energy) $E_i \geqslant 1$. At initial state, one can set randomly the height of each site in which $E_i \leqslant E_c$. E_c is the threshold height equal to the number of nearest neighbors of each site (e.g., for hypercubic lattice $E_c = 2d$). At each time step a grain is added on a randomly chosen site ($E_i \to E_i + 1$). If the height of this site exceeds E_c, a toppling occurs: $E_i \to E_i + \Delta_{i,j}$ in which $\Delta_{i,j} = -E_c$ if $i = j$, $\Delta_{i,j} = 1$ if i and j are neighbors and zero otherwise. A toppling may cause the nearest-neighbor sites to become unstable (have hight higher than E_c) and topple in their own turn and so on, until all of the lattice sites are below the critical threshold (stable state). The total process, which starts by a local perturbation (making the first site unstable) until reaching another unstable configuration, is called an avalanche. The model is conservative and the energy is dissipated only from the boundary sites. The properties of the model in $d = 2$ has been investigated extensively and well understood in the literature [33], as well as $d = 3$ [21,28,44]. The simple rule for the dynamics of the sand grains on the Ising correlated percolation lattice is that the energy is allowed to pass only through the permeable ($\sigma = +1$) sites. In fact, we use the following simple rules:

We define the Ising model on the $L \times L$ square lattice. After acquiring a spin configuration by solving the Eq. (1) for $h = 0$ at a given temperature, a spanning Ising cluster is chosen as the host media. This is defined as the connected spin cluster which contains the same spin sites and also connects opposite boundaries of the system. Let us name this host area as the *active space*. After identifying the active space, the sand grains are restricted to move on it and can be dissipated through the boundaries to which the active space is connected. Let us define the active-space coordination number as

$$z_j \equiv \sum_{i \in \text{neighbors of j}} \delta_{\sigma_i,1} + \delta_{j,\text{bndry}}, \tag{3}$$

in which δ is the Kronecker δ function and $\delta_{j,\text{bndry}}$ is unity if the site j is a boundary site and zero otherwise. Then the toppling rule for the sand grains in the site j is simply $E_j \to E_j + \Delta_{i,j}$, in which

$$\Delta_{i,j} = \begin{cases} \delta_{\sigma_j,1} & \text{if } i \text{ and } j \text{ are neighbors} \\ -z_i & \text{if } i = j \\ 0 & \text{other} \end{cases}. \tag{4}$$

The random nature of the host system implies some serious changes in the sandpile model. For the case $T \to 0$, which is the regular lattice, one retrieves the results of the ordinary BTW model.

Numerical details

At $T = T_c$ for which the Ising model becomes critical, some power-law behaviors emerge. The method to simulate the system in the vicinity of this point is important, due to the problem of critical slowing down. To avoid this problem we have used the Wolff Monte Carlo method to generate Ising samples. Our ensemble averaging contain both sandpile avalanche as well as Ising-percolation lattice averaging. For the latter case we have generated 10^2 Ising uncorrelated samples for each temperature and lattice size. To control the finite-size effects we have generated and analyzed the samples for various rates of lattice size, namely $L = 128$, 256, 512, 1024, and 2048. To make the Ising samples uncorrelated, between each successive sampling, we have implied $L^2/3$ random spin flips and let the sample to equilibrate by $500L^2$ Monte Carlo steps. The main lattice has been chosen to be square, for which the critical temperature of the Ising model is $T_c \approx 2.269$. Only the samples with temperatures $T \leqslant T_c$ have been generated, since the spanning clusters (active space) are present only for this interval. As stated in the previous section, the sand grains move only on the active space, which is defined as the set of connected sites of the same spin that connects two opposite boundaries. The temperatures considered in this paper are $T = T_c - \delta t_1 \times i$ ($i = 1,2,...,5$ and $\delta t_1 = 0.01$) to obtain the statistics in the close vicinity of the critical temperature $T_c \simeq 2.269$ (note that the model shows nontrivial power-law behaviors in the vicinity of the critical temperature) and $T = T_c - \delta t_2 \times i$ ($i = 1,2,...,10$ and $\delta t_2 = 0.05$) for the more distant temperatures. To equilibrate the Ising sample and obtain the desired samples we have started from the high temperatures ($T > T_c$). For each temperature and lattice size 10^7 avalanche samples were generated for 100 Ising samples (for each Ising sample 10^5 avalanche samples were generated and each Ising sample had its own particle dynamics to reach a steady state). We have used the Hoshen-Kopelman [45] algorithm for identifying the clusters in the lattice.

Once a spanning Ising percolation cluster (containing N active sit3ses) is obtained, the simulation of sandpiles on this cluster begins. We first attribute some random integers $\{E_i\}_{i=1}^N$ to the active sites (permeable sites whose dual spins are positive), so that $1 \leqslant E_i \leqslant 4$ and $\sigma_i = +1$. A random active site is chosen and a sand grain is added, i.e., $E_i \to E_i + 1$. If the site becomes unstable, i.e., $E_i > 4$, then it topples according to the rule Eq. (4). In this rule, the sand grains are no allowed to enter the inactive (impermeable) sites. As a results of this toppling the neighboring active sites may become unstable and topple. Therefore, a chain of topplings occurs until a stable height configuration is reached. Just like the original regular BTW model, we have transient configurations (the primitive configurations which occur in the first stages of the grain injection and do not appear again) and recurrent configurations (the configurations which occur in the steady states and repeatedly happens) here. In the transient states the average grows linearly by the number of injections, whereas for the recurrent states it is nearly constant. All of our analysis are restricted to the steady states. Figure 1 is a 512×512 sample at $T = T_c$ in which the red (white) sites show the inactive (active) sites and the set of gray sites show an avalanche which moves on the white sites. The exterior frontier of the avalanche has been identified by a black loop whose statistical properties as one of the geometrical quantity is investigated in this paper.

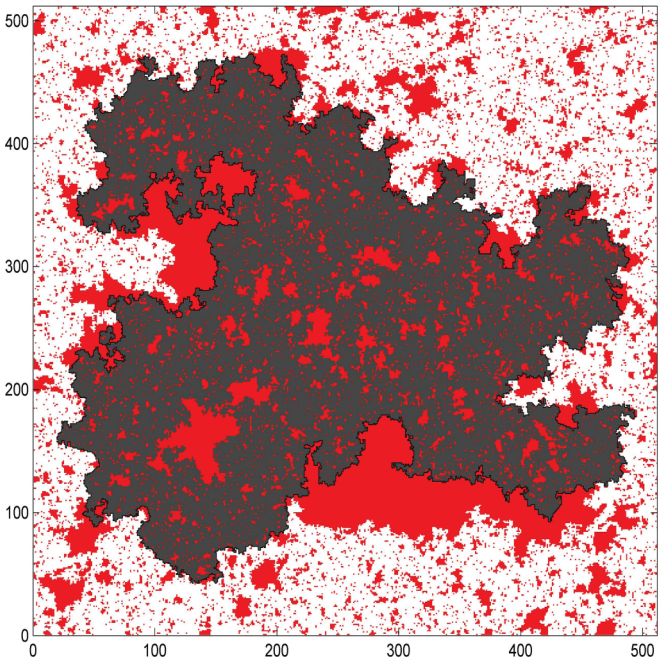

FIG. 1. A avalanche sample in an Ising sample media in a 512×512 lattice at $T = T_c$. The red sites represent the forbidden (inactive) sites, and the white sites are representative of the active ones. The toppled sites in an avalanche have been shown by the gray ones.

One of the important geometrical quantities in this paper is the spanning cluster probability (SCP) which is defined as the probability that an avalanche connects two opposite boundaries. This probability depends on the temperature (T) and the lattice size L, i.e., SCP(T,L).

The quantities studied in this paper are as follows: the number of topplings in an avalanche n; the size (mass) of the connected component of an avalanche m; the loop lengths l, which is the length of the loop that is the external perimeter of an avalanche; the loop gyration radius r, which is defined as $r^2 \equiv \frac{1}{l}\sum_{i=1}^{l}(\vec{r}_i - \vec{r}_{\rm com})^2$, which is the gyration radius of the points involved in the perimeter of the avalanche. In this formula, $\vec{r}_i$ is the position vector of the ith point and $\vec{r}_{\rm com} \equiv \frac{1}{l}\sum_{i=1}^{l}\vec{r}_i$ is the center of mass of the avalanche. It is notable that n, m, l, and r are observables related to the *size* of the avalanches.

Let us mention some points concerning the distribution functions of the statistical observables. For any critical system in the thermodynamic limit $L \to \infty$, one expects that the distribution function of any statistical observable x (=one of the observables of the above list) behaves like $P(x) \sim x^{-\tau_x}$, in which τ_x is the exponent corresponding to the observable $x = n$, m, l, and r. For the finite systems, the finite-size scaling theory predicts that [21]

$$P(x,L) = L^{-\beta_x} g_x(xL^{-\nu_x}), \tag{5}$$

in which g_x is a universal function and β and ν are the exponents corresponding to x. A simple dimensional analysis shows that $\tau_x = \frac{\beta_x}{\nu_x}$, which will be tested for all observables in the remaining of the paper. The exponent ν_x determines

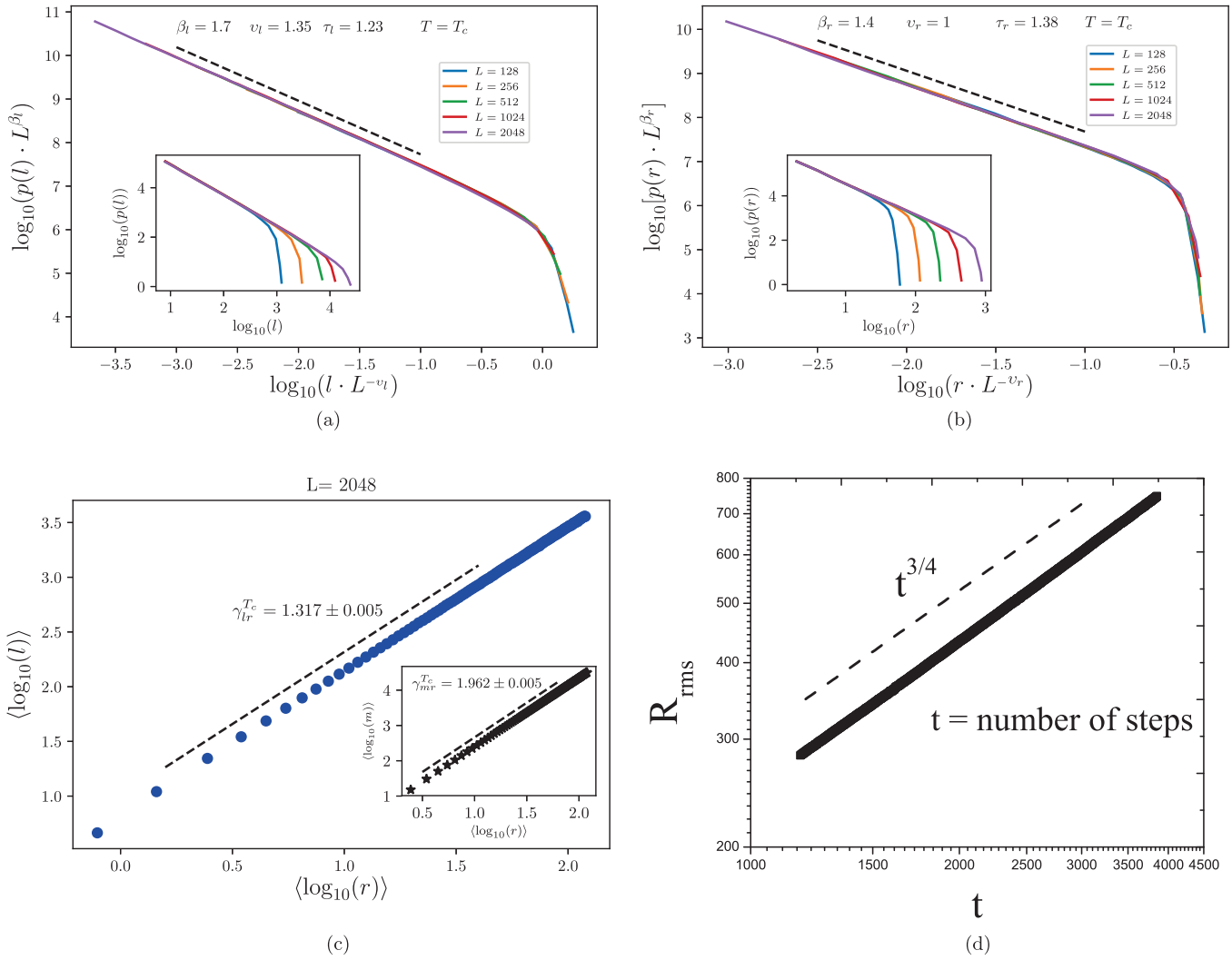

FIG. 2. The fitted plot of the distribution function of the (a) loop length (b) gyration radius with their β, ν, and τ exponents for various rates of lattice sizes. (c) The fractal dimension $D_f \equiv \gamma_{lr}$ at $T = T_c$ as the slope of the $\langle \log(l) \rangle - \langle \log(r) \rangle$ plot. Inset: the exponent γ_{mr}. (d) root-mean-square distance $R_{\rm rms}$ of the cut curves in terms of t ($t \equiv$ the *time* parametrization of the curve) with the exponent $\frac{3}{4}$ which is compatible with $\nu_{\rm SAW} = 0.75$.

the characteristic scale of the probability distribution function above which the distribution functions fall off more rapidly than a power law. If the finite-size scaling (FSS) theory works, the distributions $P_x(x, L)$ for various system sizes have to collapse to a single one, by tunning their characteristic scales. Then the argument of the universal function g has to be constant. For a critical system one may expect that the characteristic length, scale with the system size L as $r^* \sim L$, i.e., $\nu_r = 1$.

An important relation appears for the fractal dimensions defined by $y \sim x^{\gamma_{xy}}$ in which y and x are the statistical observables. In fact, using the relation $p_x(x)dx = p_y(y)dy$ for the corresponding distribution functions then leads to the scaling relation

$$\gamma_{xy} = \frac{\tau_y - 1}{\tau_x - 1}. \tag{6}$$

It is notable that this is the case only when the conditional probability $P(x|y)$ is a narrow function of both x and y. As an important example, by considering the fact that $\nu_r = 1$, after some straightforward scaling analysis one finds $\nu_x = \gamma_{xr}$ [21].

III. RESULTS

The critical behaviors of the ordinary BTW model on the regular lattice is retrieved in the limit $T \to 0$. For all temperatures in the range $T < T_c$ the critical behaviors have been observed, like the power-law behaviors as well as the FSS. We consider the critical case $T = T_c$ and $T < T_c$ separately since it is believed that there are two fixed points in the problem, namely $T = 0$ (the IR fixed point) and $T = T_c$ (the UV fixed point) [34]. In this expression we have used the terminology of the renormalization group in which the small scales are named as the *UV limit*, whereas the large scales are named as *IR limit*. The critical behaviors of the system in the vicinity of the critical temperature is reported for the maximum lattice size in this paper, i.e., $L = 2048$, although calculated for all lattice sizes.

A. Critical temperature

As stated in the previous section, the Ising model can be seen as the percolation lattice. The percolation transition in the Ising model is along with the magnetic transition, which is second order with its own critical behaviors and exponents. Our model involves some fixed points in the parameter space T. The characterization of the fixed points in any perturbed statistical models is very important, since it yields information about its large-scale behaviors. For the uncorrelated percolation lattice, it has been shown that $p = p_c$ is the UV fixed point, which is unstable toward the $p = 1$ IR fixed point [34,35]. In the renormalization group language, the properties of the BTW model on uncorrelated percolation lattice for $p > p_c$ is described by the IR fixed point in the thermodynamic limit, i.e., $p = 1$, and only the $p = p_c$ case do not run by zooming out of the system (or equivalently sending the lattice size to infinity).

In this section, we concentrate on the critical temperature case $T = T_c$. The identification of the universality class in which the model lies, in $T = T_c$, needs a detailed characterization of the model and the corresponding exponents and the finite size analysis. Due to the high diluteness of the host media, i.e., correlated percolation lattice with $T = T_c$ the number of the boundary sites from which the sand grains can dissipate is low, which causes the run time for the samples becomes large.

The first result has been shown in Fig. 2(a) in which the data collapse for the distribution function of loop lengths $p(l)$ has been sketched for various rates of lattice sizes L. We see that the graphs satisfy properly the FSS (relation 5) with $\beta_l = 1.7 \pm 0.1$ and $\nu_l = 1.35 \pm 0.1$ The slope of this graph is $\tau_l = 1.23 \pm 0.1$, which is consistent with $\tau = \frac{\beta}{\nu}$, which is necessary for the FSS hypothesis. This exponent is far from the same exponent for the geometrical spin clusters for the Ising model, i.e., $\tau_l^{\text{Ising}} \simeq 2.75$ [9], but is close to the exponent for the 2D BTW model $\tau_l^{\text{2DBTW}} \simeq 1.28$ [46]. In this sense our model is something between the Ising model and the 2D BTW models. The same analysis for the gyration radius of loops yields $\beta_r = 1.4 \pm 0.1$, $\nu_r = 1 \pm 0.01$, and $\tau_r = 1.38 \pm 0.02 \approx \frac{\beta_r}{\nu_r}$. For the comparison, we note that $\tau_r^{\text{2DBTW}} \simeq \frac{5}{3}$ [21] and $\tau_l^{\text{Ising}} \simeq 3.4$ [13]. The fact that $\nu_r = 1$ is expected and signals the fact that the characteristic radius scales linearly with the system size L which is a property of the critical systems.

The more important exponent in this system is γ_{lr}, which is known as the fractal dimension of the loops, sometimes represented by D_f. The importance of this exponent has roots in its relation to the diffusivity parameter (κ) in the Schramm-Loewner evolution (SLE) theory [47,48]. SLE$_\kappa$ aims to classify the 2D critical models into one parameter classes, which are identified by κ [48]. It is well-known that there is a deep connection between this parameter and D_f, via the relation $D_f = 1 + \frac{\kappa}{8}$. Therefore, one may interpret this as the fact that the 2D statistical models can be classified via the determination of D_f. In fact, there are some other measures for identifying the diffusivity parameter via winding angle statistics [48], left passage probability [49,50] and direct SLE mapping [51,52]. Since the determination of D_f is one of the most reliable methods, we have calculated it as precisely as possible. The result has been shown in Fig. 2(c) for various system sizes. The size dependence of this exponent also appears in the inset of Fig. 4(a), which will be described in the next section. The analysis of the slope in this figure shows that $D_f = 1.317 \pm 0.005$. The most compatible fractional value to this result is $\frac{4}{3}$, which corresponds to the SLE universality class $\kappa = \frac{8}{3}$. This is the universality class of self-avoiding walk (SAW) whose fractal dimension is $D_f^{\text{SAW}} = \frac{4}{3} \simeq 1.33$. In the inset of this figure, γ_{mr} has been shown to be 1.962 ± 0.005. This amount is apparently lower that $\gamma_{mr}^{\text{2DBTW}} = 2$ for the BTW model on the regular 2D lattice. This is because of the presence of impermeable (inactive) sites inside the avalanches which cause it to be less compact than the regular case in which no hallow is present.

To be more precise, we have also calculated a more direct measure for testing the SAW. It is well-known that for a 2D SAW which starts from the origin and ends on an arbitrary point on the boundary, the distance R_{rms} (= root-mean-square distance) as a function of the number of taken steps t (which is referred to as the time) scales as $R_{\text{rms}} \sim t^{\nu_R}$ in which $\nu_R = 0.75$. To test this in our case we should force the stochastic path to start from the boundary and end on a uniformly random chosen point on the boundary. To this end we use the common strategy in the loop analysis of 2D critical systems [46,51]. In this approach one cuts the loops by a horizontal line (along the x or y axis), which passes the center of mass of the loop and sends its end point to a uniformly random chosen point at infinity. Suppose that the curve path composed of N points is $\{0, Z_1, Z_2, Z_3, ..., Z_N\}$, in which $Z_i \equiv x_i + iy_i$ is the position of the ith point in the upper half plane and $Z_N = x_N$ shows that the curve ends on the real axis. Then the map $W_i \equiv x_N \frac{Z_i}{Z_i - x_N}$ transforms the curve to the one that goes from the origin to a random point at infinity. After this process, one can plot ensemble averaged R in terms of the number of steps to extract the corresponding ν_R. To avoid any possible statistical error the walk is truncated if the length of the single walk become more that a threshold which has been set to 10 in our case. The result has been shown in Fig. 2(d) in which R_{rms} has been drawn in terms of t in a log-log plot. It is seen that $\nu_R = 0.78 \pm 0.05$, which is in agreement with the result of SAW.

Before closing this section let us mention some points concerning the conformal Mobius map $w(Z)$, which has been introduced above. In general, one may expect that the fractal dimension of *free* SAW is the inverse of ν_R by some scaling arguments. The above results show that the statistical properties of the random curves has not been changed by applying the $w(Z)$ map. It is the finger print of the conformal invariance of the model in hand, since after a this Mobius map the properties of the original model and the mapped model is not changed. One concludes that at $T = T_c$ the model has conformal invariance.

B. Off-critical temperatures

In this section we consider the problem in the more general case, i.e., all temperatures involved. This study is more interesting since it shows the total structure of the system in hand. The exponents have been reported for the maximum system size ($L = 2048$) in this section. The finite-size dependence of the exponents are also reported. For a single lattice size the exponents of the distribution functions

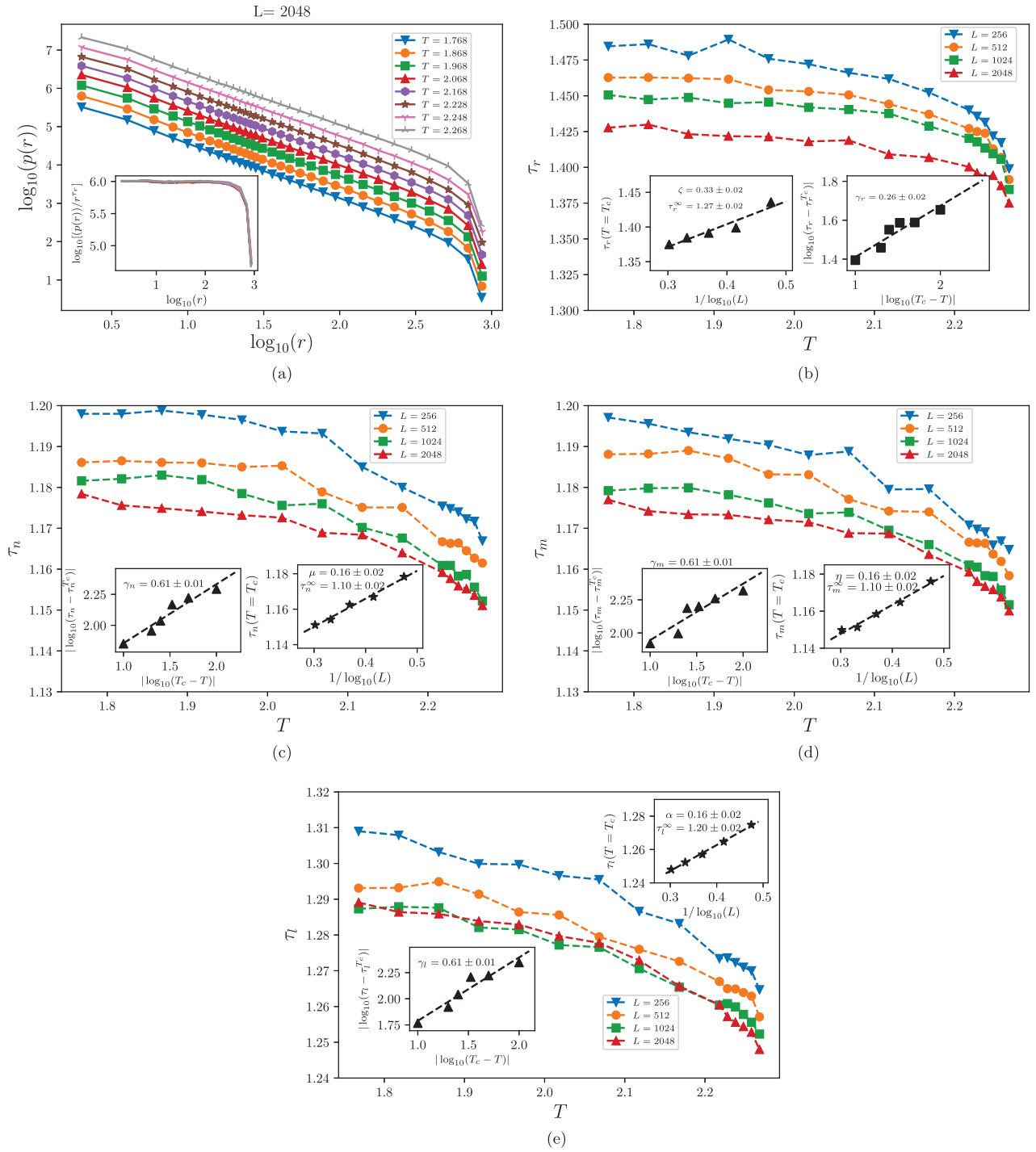

FIG. 3. (a) The plot of the distribution function of the gyration radius for various rates of the temperature T. Inset: the collapse graphs of the main graph. The exponents of the distribution functions of (b) the gyration radius r (c) the number of topplings in an avalanche n, (d) the mass of the avalanches m, and (e) the loop length l length of the frontier of avalanche in terms of T for various system sizes. Insets: The linear fits of the exponents at $T = T_c$ in terms of $1/\log(L)$, L being the lattice size, from which the thermodynamic values can be extrapolated, and the power-law behaviors of exponents near the critical temperatures with the exponents represented by γ_x ($x \equiv r, n, m$, and l).

have been calculated by the linear fitting of the log-log plot of the figures. For distinguishing the linear part of the graph, we have used the R^2 test. The linear part of each graph has been determined up to a scale above which the R^2 of the linear fit becomes less than 0.99. One may be concerned about the criticality of the system in these off-critical temperatures. In fact, we have observed that for all temperatures in this interval the system shows power-law behaviors with some well-defined exponents. We notice that at $T = 0$ the regular BTW model is obtained which is critical. Our observations support the fact that the exponents are rapidly saturated and become nearly constant with small fluctuations for low-temperatures towards

TABLE I. The exponents of distribution functions of $x = n, m, l$, and r at model $T = T_c$. The first column shows the thermodynamic value of the exponents, obtained form finite-size analysis. The last two columns show the corresponding values for the 2D BTW and Ising models for comparison. The data for the BTW has been written from Ref. [21], and the data for the Ising model has been written from Ref. [52].

	$\tau^{L\to\infty}$	$\tau^{L=2048}$	ν	β	$\frac{\beta}{\nu}$	τ_{2DBTW}	τ_{Ising}
n	1.1(2)	1.15(2)	1.1(2)	1.27(2)	1.15(2)	1.293	–
m	1.1(2)	1.15(2)	1.11(2)	1.28(2)	1.15(2)	$\frac{4}{3}$	3.31
l	1.2(2)	1.23(1)	1.35(1)	1.7(1)	1.25	1.28	2.75
r	1.27(2)	1.38(2)	1.0(1)	1.4(1)	1.4	$\frac{5}{3}$	3.4

the $T = 0$ results. This behavior is stronger for larger lattice sizes which shows that the dominant behavior of the system is that of $T = 0$ case in the thermodynamic limit for $T < T_c$. The distribution function of the gyration radius for various rates of temperature T has been shown in Fig. 3(a). As is seen the slopes change slightly by varying T. In the inset the collapsed graphs have been shown. The corresponding exponents have been appeared in Fig. 3(b) for various rates of lattice sizes. The exponents monotonically decrease from 1.43 ± 0.02 for low temperature to 1.37 ± 0.02 for $T = T_c$ and $L = 2048$. The dashed line has been drawn for helping eye. As is seen in this figure the data points for the temperatures near the critical one is considered to be more than others to track the power-low behaviors in this interval. The left inset shows the finite-size amounts of the exponent at $T = T_c$. A good linear behavior is seen with respect to $1/(\log_{10}(L))$. In fact, we see that

$$\tau_x(L, T = T_c) = \tau_x(L = \infty, T = T_c) + \frac{a_x}{\log_{10}(L)} \qquad (7)$$

for all x's, namely, $x = n, m, l$, and r, and $\tau_x(L = \infty, T = T_c)$ and a_x are the fitting parameters to be determined. The parameters of this equation have been obtained using the least squares estimator (LSE) method. The dependence to $\frac{1}{\log_{10}(L)}$ has also previously seen for regular BTW models [21]. $\tau_x(L = \infty, T = T_c)$ is interpreted as the thermodynamic value of the exponents which have been reported in the Table I. The other exponents have been shown in Figs. 3(c)–3(e) in which $\mu \equiv a_n$, $\eta \equiv a_m$, $\alpha \equiv a_l$, and $\zeta \equiv a_r$ that are of the secondary importance in our analysis. It is seen that τ_n and τ_m are nearly the same in contrast to the regular 2D BTW model. Note that for the three- and four-dimensional BTW model τ_m and τ_n are approximately equal. The equality of these exponents reflects the fact that avalanches and the waves are the same. More precisely, in a single avalanche, each site maximally topples one time; i.e., no site can topple more than one time. It is interesting that this is also the case for the system in hand, i.e., BTW on the Ising-diluted square lattice for which the fractal dimension is lower than two.

The behavior of the model in the vicinity of the critical temperature is also seen to be power-law. The corresponding analysis has been performed for $L = 2048$ in the mentioned figures. The observed power-law behaviors are described by the following relation:

$$|\tau_x(T) - \tau_x(T_c)| \propto |T - T_c|^{\gamma_x}, \qquad (8)$$

TABLE II. The exponents of the off-critical temperature. The second row shows the closest fractional values.

	γ_n	γ_m	γ_l	γ_r	κ_{lr}	κ_{mr}
Exponent	0.48(1)	0.61(1)	0.61(1)	0.26(2)	0.47(3)	0.82(2)
Fractional val.	$\frac{1}{2}$	$\frac{3}{5}$	$\frac{3}{5}$	$\frac{1}{4}$	$\frac{1}{2}$	$\frac{4}{5}$

in which γ_x is the corresponding exponent. The numerical values of the exponents have been presented in Table II. The fractional values are $\gamma_n \simeq 2\gamma_r \simeq \frac{1}{2}$ and $\gamma_m \simeq \gamma_l \simeq \frac{3}{5}$.

The same analysis has been done for the fractal dimensions which has been presented in Figs. 4(a) and 4(b) for various system sizes. We see that γ_{lr} is an increasing function of T starting at $\gamma_{lr}^{T=0} \simeq 1.25$ (compatible with regular BTW model) and ending at $\gamma_{lr}^{T=T_c} \simeq 1.32$, whereas γ_{mr} is decreasing function starting at $\gamma_{mr}^{T=0} \simeq 2$ (compatible with the regular BTW model) and ending at $\gamma_{mr}^{T=T_c} \simeq 1.96$. The finite-size dependence of the exponents has been shown in the lower insets. Interestingly, we have observed that the fractal dimensions scale with $\frac{1}{L}$ in sharp contrast to the $\frac{1}{\log_{10}(L)}$ for the exponents of the distribution functions presented above. In fact, for the fractal dimensions the relation is

$$\gamma_{xy}(L) = \gamma_{xy}(L = \infty) + \frac{\sigma_{xy}}{L}, \qquad (9)$$

in which $\gamma_{xy}(L = \infty)$ and σ_{xy} are the fitting parameters. We see that $\gamma_{lr}^{L=\infty, T=T_c} = 1.32 \pm 0.005$ and $\gamma_{mr}^{L=\infty, T=T_c} = 1.96 \pm 0.005$. Also in the vicinity of the critical temperature we see that the following relation is satisfied:

$$\left|\gamma_{xy}(T) - \gamma_{xy}(T_c)\right| \propto |T - T_c|^{\kappa_{xy}}, \qquad (10)$$

in which κ_{xy} is its exponent. From the upper insets of these figures we see that $\kappa_{lr} \simeq \frac{1}{2}$ and $\kappa_{mr} \simeq \frac{4}{5}$. Before further analysis let us present some scaling arguments concerning the fractal dimension of loops $D_f(T)$ and the exponent $\tau_l(T)$. Let us abbreviate $l_T(r) \equiv \langle l(r)\rangle|_T$. From the scaling relation $\frac{l_T(r)}{l_{T_c}(r)} = r^{D_f(T) - D_f(T_c)}$ one easily finds that $l_{T_c} = l_T^{2 - \frac{D_f(T)}{D_f(T_c)}}$. Using this, and the the equality of the distribution probabilities $(p_T(l)dl_T = p_{T_c}(l)dl_{T_c})$ we obtain

$$p_T(l) = p_{T_c}(l)\frac{dl_{T_c}}{dl_T} = p_{T_c}(l)\left[2 - \frac{D_f(T)}{D_f(T_c)}\right] l_T^{1 - \frac{D_f(T)}{D_f(T_c)}}. \qquad (11)$$

Using the fact that $p_T(l) \sim l^{-\tau_l(T)}$ and $p_{T_c}(l) \sim l^{-\tau_l(T_c)}$ one finally finds that

$$\tau_l(T) - \tau_l(T_c) = \left[\frac{\tau_l(T_c) - 1}{D_f(T_c)}\right][D_f(T_c) - D_f(T)], \qquad (12)$$

showing that the exponents κ_{lr} and γ_l should be the same. The 23% discrepancy is due to the fact that the relation $p_T(l)dl_T = p_{T_c}(l)dl_{T_c}$ is not that exact, since p's belong to different samplings. The power-law behavior in the vicinity of the critical temperature has been gathered in the Table II.

The other important test is the hyper-scaling relation 6 which is investigated for $T = T_c$ for γ_{lr} and γ_{mr}. The total information concerning these exponents has been shown in Table III. For the comparison the corresponding exponents for the regular 2D BTW and 2D Ising models have been shown in

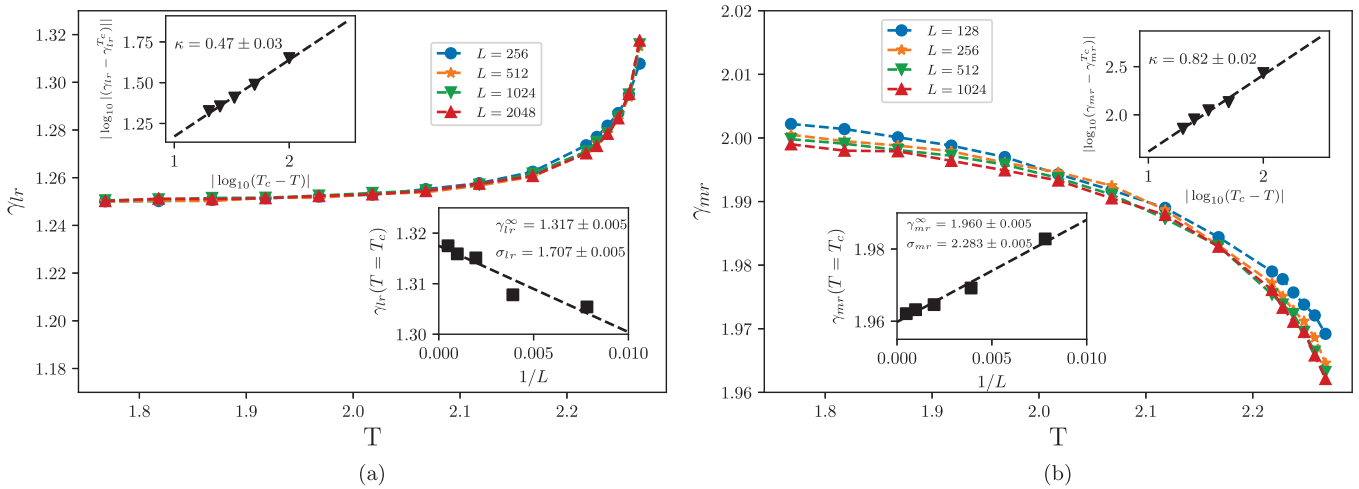

FIG. 4. (a) The γ_{lr} and (b) the γ_{mr} in terms of T for various system sizes. The lower insets show the finite-dependence of the exponents in terms of $1/L$ at $T = T_c$, L being the system size, from which the thermodynamic values can be extrapolated. The upper insets show the power-law behavior of the exponents in the vicinity of the critical temperature with the exponents shown by κ.

this table. The numerical values of the exponents are between the corresponding exponents of BTW and Ising models, e.g., $\gamma_{mr}^{\text{2DIsing}} \simeq 1.85 < \gamma_{mr} \simeq 1.96 < \gamma_{mr}^{\text{2DBTW}} = 2$.

An interesting question in this system is the following: What is the probability that an avalanche connects two opposite boundaries, i.e., percolates? It is the spanning cluster probability (SCP). This probability is a measure of how the particles are free to reach the boundaries and how large the avalanches can be. These probabilities have been drawn in Fig. 5 as a function of T and L. For each amount of L, SCP is nearly constant for the most (low) temperature interval and decreases as the temperature approaches T_c from below. In the vicinity of T_c, SCP behaves in a power-law fashion, but due to large statistical fluctuations, we could not extract the exponent. The L dependence at $T = T_c$ is, however, power law with a well-defined exponent. As is seen in this figure SCP is a decreasing function of L for all temperatures. In the left inset of this figure we have shown the plot of $\log_{10}\text{SCP}(T = T_c, L)$ in terms of $\log_{10} L$ from which it is seen that $\text{SCP}(T = T_c, L) \sim L^{-\gamma_p}$ with $\gamma_p \simeq \frac{1}{2}$. For the comparison we have also calculated the same for the low temperatures which has been shown in the right inst for $T = 1.768$, from which we see a same dependence on L with the exponent $\gamma_p(T = 1.768) = 0.42 \pm 0.02$, which is an estimation for the regular BTW model. Therefore, this exponent is different from the regular BTW model.

We close this section by concluding that the behavior of the statistical observables near the critical temperature is power law. The exponents of the distribution functions are linear with respect to $1/\log_{10} L$, whereas the fractal dimensions are linear with respect to $1/L$ and $\text{SCP}(T = T_C, L) \sim L^{\frac{1}{2}}$.

TABLE III. The fractal dimensions (γ_{lr} and γ_{mr}) of the model. The last two columns show the corresponding values for the 2D BTW and Ising models for comparison. The second row shows the obtained values from hyperscaling relation.

	$\gamma_{lr}^{L\to\infty}$	$\gamma_{lr}^{\text{2DBTW}}$	$\gamma_{lr}^{\text{Ising}}$	$\gamma_{mr}^{L\to\infty}$	$\gamma_{mr}^{\text{2DBTW}}$	$\gamma_{mr}^{\text{2DIsing}}$
Num. value	1.32(1)	$\frac{5}{4}$	$\frac{11}{8}$	1.96(1)	2	1.85
$\gamma_{xy}^{\text{h.s.}} \sim \frac{\tau_y - 1}{\tau_x - 1}$	1.34	—	—	1.93	—	—

IV. DISCUSSION AND CONCLUSION

Many features of the sandpile models on the random fractal lattices are known. Since these host systems are commonly considered to be uncorrelated, introducing correlation in them is important and interesting and is shown to have nontrivial effects. In this paper, we have considered the BTW-type sandpile model on the Ising-correlated porous media whose correlations are controlled by an artificial temperature T.

At $T = T_C$ the statistical properties of the self-avoiding walk has emerged, mainly the fractal dimension of the external frontiers of the avalanches are like self-avoiding walks with $D_f = \frac{4}{3}$. Applying a conformal transformation of the cut curves reveals that $R_{\text{rms}} \sim t^{\nu}$ with $\nu = 3/4$ and t being the

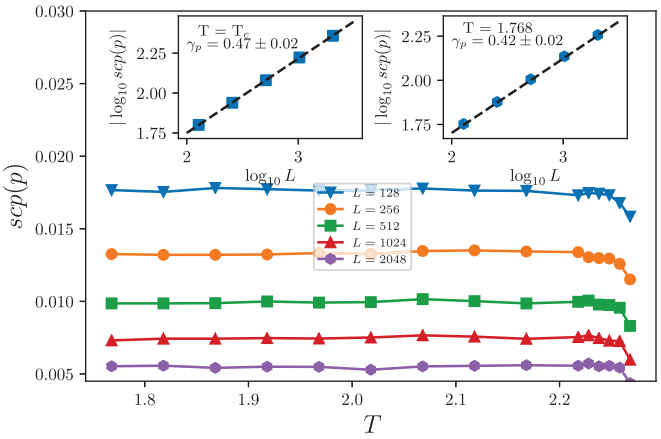

FIG. 5. The spanning cluster probability $\text{SCP}(T, L)$ in terms of T for various rates of lattices sizes. The inset shows the power-law behavior of this function in terms of L at the critical temperature with the exponent $\frac{1}{2}$.

parametrization (time) of the curve, in agreement with SAW. The fact that $\nu = 1/D_f$ shows that the curves at $T = T_C$ *have conformal invariance*. We conclude that introducing the Ising-like site-dilution causes the $c = -2$ CFT (BTW fixed point) to cross to the $c = 0$ CFT (SAW fixed point). The result that at $T = T_c$ the exponents of the distribution functions are linear with respect to $1/\log L$ (as the famous feature of the regular BTW model), whereas the fractal dimensions are linear with respect to $1/L$ (like the regular Ising model), shows that our model is an intermediate one between the regular BTW and the critical Ising models. One of the most important findings of the present work is the fact that $\mathrm{SCP}(T = T_c, L) \sim \sqrt{L}$, which should be compared with the result for the low temperature result (corresponding to the 2D regular BTW model), which is $\mathrm{SCP}(\text{low } T, L) \sim L^{0.42\pm0.02}$. This shows that the rate of the fluid (oil) production depends on the square root of the linear extent of a reservoir, and when the correlations weaken, then this dependence also weakens; i.e., the correlations favor the lower extent of the fluid propagation.

To conclude, our results show that at $T = T_c$ the properties of the model is most compatible with SAW. Finite-size scaling theory has also been shown to be fulfilled for all of the observables investigated in this paper. Importantly, it is seen that some exponents act like the BTW and some like the 2D critical Ising model, showing that the model is interpolation between these models. The statistical observables show also power-law behaviors in terms of $T - T_C$ in the vicinity of the critical temperature with well-defined exponents, which was reported in the text. The fact that spanning cluster probability scales with $\sqrt{L}$ is of practical importance, since it is directly related to the fluid production in the petroleum engineering.

ACKNOWLEDGMENT

We thank the anonymous referees for their helpful comments and detailed analysis.

[1] Y. Gefen, B. B. Mandelbrot, and A. Aharony, Phys. Rev. Lett. **45**, 855 (1980).
[2] A. R. Kose, B. Fischer, L. Mao, and H. Koser, Proc. Natl. Acad. Sci. USA **106**, 21478 (2009).
[3] H. Kikura, J. Matsushita, M. Matsuzaki, Y. Kobayashi, and M. Aritomi, Sci. Technol. Adv. Mater. **5**, 703 (2004).
[4] M. Matsuzaki, H. Kikura, J. Matsushita, M. Aritomi, and H. Akatsuka, Sci. Technol. Adv. Mater. **5**, 667 (2004).
[5] J. Philip, P. Shima, and B. Raj, Appl. Phys. Lett. **91**, 203108 (2007).
[6] J. H. Kim, F. F. Fang, H. J. Choi, and Y. Seo, Mater. Lett. **62**, 2897 (2008).
[7] P. Y. Keng, B. Y. Kim, I.-B. Shim, R. Sahoo, P. E. Veneman, N. R. Armstrong, H. Yoo, J. E. Pemberton, M. M. Bull, J. J. Griebel *et al.*, ACS Nano **3**, 3143 (2009).
[8] H. Kikura, J. Matsushita, N. Kakuta, M. Aritomi, and Y. Kobayashi, J. Mater. Process. Technol. **181**, 93 (2007).
[9] M. Najafi, Phys. Lett. A **380**, 370 (2016).
[10] W. Li, J. L. Jensen, W. B. Ayers, S. M. Hubbard, and M. R. Heidari, J. Petrol. Sci. Eng. **68**, 180 (2009).
[11] A. D. Araújo, T. F. Vasconcelos, A. A. Moreira, L. S. Lucena, and J. S. Andrade, Jr., Phys. Rev. E **72**, 041404 (2005).
[12] C. Oliveira, A. Araújo, L. Lucena, M. Almeida, and J. Andrade, Physica A **391**, 3219 (2012).
[13] M. Najafi and M. Ghaedi, Physica A **427**, 82 (2015).
[14] B. C. Craft, M. F. Hawkins, and R. E. Terry, *Applied Petroleum Reservoir Engineering*, Vol. 9 (Prentice-Hall, Englewood Cliffs, NJ, 1959).
[15] J. M. Beggs and D. Plenz, J. Neurosci. **23**, 11167 (2003).
[16] M. Najafi, Phys. Lett. A **378**, 2008 (2014).
[17] M. Najafi and H. Dashti-Naserabadi (unpublished).
[18] P. Bak, C. Tang, and K. Wiesenfeld, Phys. Rev. Lett. **59**, 381 (1987).
[19] P. Bak, C. Tang, and K. Wiesenfeld, Phys. Rev. A **38**, 364 (1988).
[20] D. Sornette, *Critical Phenomena in Natural Sciences: Chaos, Fractals, Self-organization and Disorder: Concepts and Tools* (Springer Science & Business Media, Berlin, 2004).
[21] S. Lübeck and K. D. Usadel, Phys. Rev. E **56**, 5138 (1997).
[22] D. Dhar, Physica A **263**, 4 (1999).
[23] V. Priezzhev, J. Stat. Phys. **98**, 667 (2000).
[24] M. De Menech and A. L. Stella, Phys. Rev. E **62**, R4528 (2000).
[25] S. N. Majumdar and D. Dhar, J. Phys. A: Math. Gen. **24**, L357 (1991).
[26] E. V. Ivashkevich, D. V. Ktitarev, and V. B. Priezzhev, Physica A **209**, 347 (1994).
[27] D. Dhar and S. S. Manna, Phys. Rev. E **49**, 2684 (1994).
[28] D. V. Ktitarev, S. Lübeck, P. Grassberger, and V. B. Priezzhev, Phys. Rev. E **61**, 81 (2000).
[29] S. Majumdar and D. Dhar, Physica A **185**, 129 (1992).
[30] S. Mahieu and P. Ruelle, Phys. Rev. E **64**, 066130 (2001).
[31] H. Saleur and B. Duplantier, Phys. Rev. Lett. **58**, 2325 (1987).
[32] A. Coniglio, Phys. Rev. Lett. **62**, 3054 (1989).
[33] D. Dhar, Physica A **369**, 29 (2006).
[34] M. Najafi, M. Ghaedi, and S. Moghimi-Araghi, Physica A **445**, 102 (2016).
[35] M. Najafi, J. Phys. A: Math. Theoret. **49**, 335003 (2016).
[36] D. Wilkinson and J. F. Willemsen, J. Physics A: Math. Gen. **16**, 3365 (1983).
[37] H. Auradou, K. J. Måløy, J. Schmittbuhl, A. Hansen, and D. Bideau, Phys. Rev. E **60**, 7224 (1999).
[38] M. A. Knackstedt, A. P. Sheppard, and W. V. Pinczewski, Phys. Rev. E **58**, R6923(R) (1998).
[39] R. E. Terry, J. Brandon Rogers, and B. Cole Craft, *Applied Petroleum Reservoir Engineering* (Pearson Education, 2013).
[40] A. B. Zamolodchikov, JETP Lett. **43**, 730 (1986).
[41] G. Delfino, Nucl. Phys. B **818**, 196 (2009).
[42] S. Fortunato, Phys. Rev. B **66**, 054107 (2002).
[43] S. Fortunato, Phys. Rev. B **67**, 014102 (2003).
[44] H. Dashti-Naserabadi and M. N. Najafi, Phys. Rev. E **91**, 052145 (2015).
[45] J. Hoshen and R. Kopelman, Phys. Rev. B **14**, 3438 (1976).
[46] M. N. Najafi, S. Moghimi-Araghi, and S. Rouhani, Phys. Rev. E **85**, 051104 (2012).

[47] O. Schramm, Isr. J. Math. **118**, 221 (2000).
[48] J. Cardy, Ann. Phys. **318**, 81 (2005).
[49] M. N. Najafi, Phys. Rev. E **87**, 062105 (2013).
[50] M. N. Najafi, Phys. Rev. E **92**, 022113 (2015).
[51] M. Najafi, S. Moghimi-Araghi, and S. Rouhani, J. Phys. A: Math. Theoret. **45**, 095001 (2012).
[52] M. Najafi, J. Stat. Mech.: Theor. Exp. **2015**, P05009 (2015).